Reprint from *Journal of Robotic Systems*, Vol. 12, No. 4, April 1995, pp. 257-273,

Internal Correction of Dead-reckoning Errors With a Dual-drive Compliant Linkage Mobile Robot

by
Johann Borenstein
The University of Michigan
Department of Mechanical Engineering and Applied Mechanics
1101 Beal Avenue
Ann Arbor, MI 48108
Ph.: (313) 763-1560, Fax: (313) 971-2475
Email: johannb@umich.edu

ABSTRACT

This paper presents ***I**nternal **P**osition **E**rror **C**orrection* (IPEC) — a new method for accurate and reliable dead-reckoning with mobile robots. The IPEC method has been implemented on our recently developed ***M**ulti-**D**egree-**o**f-**F**reedom* (MDOF) mobile platform, a vehicle in which two differential-drive mobile robots (called "trucks") are physically connected through a *compliant linkage*. In addition to its four wheel encoders, the MDOF platform has one linear and two rotary *internal* encoders, which allow measurement of the relative distance and bearing between the two trucks. During operation, both trucks perform conventional dead-reckoning with their wheel encoders. But, in addition, the IPEC method uses information from the internal encoders to detect and correct dead-reckoning errors as soon as they occur.

Our system, called ***C**ompliant **L**inkage **A**utonomous **P**latform with **P**osition **E**rror **R**ecovery* (CLAPPER), requires neither external references (such as navigation beacons, artificial landmarks, known floorplans, or satellite signals), nor inertial navigation aids (such as accelerometers or gyros). Nonetheless, the experimental results included in this paper show one to two orders of magnitude better positioning accuracy than systems based on conventional dead-reckoning. The CLAPPER corrects not only systematic errors, such as different wheel diameters, but also non-systematic errors, such as those caused by floor roughness, bumps, or cracks in the floor.

These features are made possible by exploiting the new ***Growth-Rate Concept*** for dead-reckoning errors that is introduced in this paper for the first time. The *Growth-Rate Concept* distinguishes between certain dead-reckoning errors that develop slowly while other dead-reckoning errors develop quickly. Based on this concept, truck A frequently measures a property with *slow-growing* error characteristics on reference truck B (thus admitting a small error) to detect a *fast-growing* error on truck A (thus correcting a large error), and vice versa.

1. INTRODUCTION

In most mobile robot applications two basic position-estimation methods are employed together: *absolute* and *relative* positioning [Borenstein and Koren, 1987; Hongo et al, 1987]. Relative positioning is usually based on dead-reckoning (i.e., monitoring the wheel revolutions to compute the offset from a known starting position). Dead-reckoning is simple, inexpensive, and easy to accomplish in real-time. The disadvantage of dead-reckoning is its unbounded accumulation of errors. One approach aiming at overcoming this problem without external references was tested in simulations by Kurazume and Nagata [1994]. This approach uses multiple cooperating mobile robots divided into two groups. When the members of group A move, the members of group B remain stationary and provide positioning beacons that the group A robots can use for absolute positioning. After a while, group A robots stand and group B robots move. Our group here at the Mobile Robotics Lab had proposed similar systems in the past, but we found that the new method described in this paper is substantially more versatile because it allows dead-reckoning error correction while the vehicle(s) is (are) in full motion.

Absolute positioning methods usually rely on (a) navigation beacons, (b) active or passive landmarks, (c) map matching, or (d) satellite-based navigation signals. Each of these absolute positioning approaches can be implemented by a variety of methods and sensors. Yet, none of the currently existing systems is particularly elegant. Navigation beacons and landmarks usually require costly installations and maintenance, while map-matching methods are either very slow or inaccurate [Cox, 1991; Schiele and Crowley, 1994], or even unreliable [Congdon et al, 1993]. With any one of these measurements it is necessary that the work environment either be prepared or be known and mapped with great precision. Satellite-based navigation can be used only outdoors and has poor accuracy (on the order of several meters) when used in real-time, during motion [Byrne, 1993, Everett, 1995].

Another approach to the position determination of mobile robots is based on inertial navigation with gyros and/or accelerometers. Our own experimental results with this approach, as well as the results published by Barshan and Durrant-Whyte [1993], indicate that this approach is not advantageous. Accelerometer data must be integrated twice to yield position, thereby making these sensors exceedingly sensitive to *drift*. Another problem is that accelerations under typical operating conditions can be very small, on the order of 0.01 g. Yet, fluctuations of this magnitude already occur if the sensor tilts relative to a perfectly horizontal position by only 0.5 ^{o}, for example when the vehicle drives over uneven floors. Gyros can be more accurate (and costly) but they provide information only on the rotation of a vehicle. Recently introduced laser gyros and optical fiber gyros promise better accuracy, low drift, and reasonable prices. However, a potentially grave problems with such gyros is that they have a minimum detectable rate of rotation: If a mobile robot has a lower rate of rotation (as may easily be the case for a robot that is supposed to travel straight, but, due to unequal wheel diameters, travels along a slightly curved path), then the gyro will not register this rotation at all [Borenstein and Feng, 1995, Everett, 1995].

Accurate dead-reckoning is particularly important in mobile robot-based map-building. Map-building has long been a popular subject of mobile robotics research. Ideally, a map-building mobile robot can be "set loose" in an unknown environment, will then roam about for some time while sensing the location of walls and other objects, and will finally return to the starting position with a detailed map of the environment. Research in map-building focuses on the problem of sensing objects and determining the boundaries of objects relative to the mobile robot. Typically, little or no attention is paid to the problem of knowing the exact location of the robot itself. Yet, the resulting maps cannot be accurate if the position of the robot is not known. It is further obvious that in an unknown environment accurate positioning of the robot by means of navigation beacons or feature matching are not applicable, leaving dead-reckoning as the only feasible choice for determining the position of the robot. However, dead-reckoning is well known to be inaccurate with an unbounded accumulation of errors. Typical dead-reckoning errors will become so large that the robot's internal position estimate is totally wrong (and certainly unsuitable for map-building) after as little as 10 m of travel [Gourley and Trivedi, 1994].

Other important applications for accurate dead-reckoning are those where the floor in the work area cannot be *guaranteed* to be smooth and free of debris. Examples are construction sites, agricultural installations, and most outdoor applications.

This paper introduces a new method for correcting dead-reckoning errors without external references. This method, called ***I**nternal **P**osition **E**rror **C**orrection* (IPEC), requires two collaborating mobile robots that can accurately measure their relative distance and bearing during motion. Our previously developed MDOF vehicle [Borenstein, 1993; 1994a] meets these requirements and we were able to implemented and test the IPEC method on this vehicle with only minor modifications. Because of the new error correction capability, we now call our vehicle the ***C**ompliant **L**inkage **A**utonomous **P**latform with **P**osition **E**rror **R**ecovery* (CLAPPER) [Borenstein, 1994b]. Section 2 summarizes the relevant characteristics of the MDOF vehicle. Section 3 analyses the nature of dead-reckoning errors and introduces the new *Growth-Rate Concept* for dead-reckoning errors. The IPEC method makes extensive use of this concept, as explained in Section 4. Section 5 discusses additional issues related to systematic dead-reckoning errors, and Section 6 presents extensive experimental results.

2. THE MDOF COMPLIANT LINKAGE VEHICLE

In previous research we have developed an innovative *Multi-Degree-of-Freedom* (MDOF) vehicle with *compliant linkage* (Fig. 1). The advantage of MDOF vehicles over conventional mobile robots is that they can travel sideways and they can negotiate tight turns easily. However, existing MDOF vehicles have been found difficult to control because of their overconstrained nature [Moravec, 1984; Reister, 1991]. These difficulties translate into severe wheel slippage or jerky motion under certain driving conditions, as evident from the poor dead-reckoning accuracy of some MDOF vehicles reported by Reister [1991], Killough and Pin [1992], West and Asada [1992], Hirose and Amano [1993], or Pin and Killough [1994]. Because of this problem MDOF vehicles are not very suitable for mobile robot applications that rely heavily on dead-reckoning. It should be noted that Reister and Unseren [1993] developed a *Force Control Method* for their two-wheel drive/two-wheel steer platform, which resulted in a reported 20-fold improvement of accuracy. However, the experiments on which these results were based avoided *simultaneous* steering and driving of the two steerable drive wheels. This

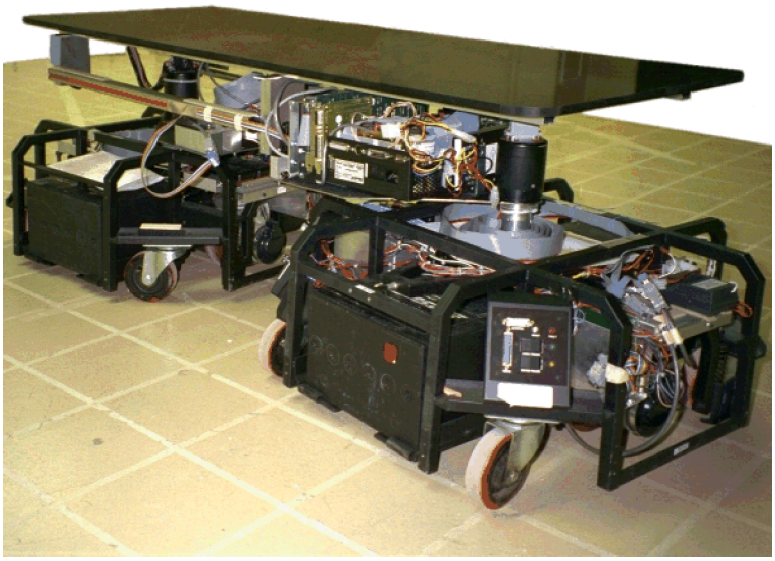

Figure 1: The University of Michigan's experimental dual differential drive vehicle with compliant linkage.

way, the critical problem of coordinating the control of all four motors *simultaneously and during transients* was completely avoided.

Our MDOF vehicle overcomes these difficulties by introducing the *compliant linkage* design (Fig. 2). The compliant linkage accommodates momentary controller errors and thereby successfully eliminates the *excessive* wheel slippage reported by other makers of MDOF vehicles.

The schematic drawing in Fig. 2 shows the essential components of the compliant linkage vehicle. The vehicle comprises of two trucks (in our prototype, these are commercially available *LabMate* robots from TRC [1993]). The two trucks are connected by the compliant linkage, which allows almost force-free relative motion within its physical range (the frictional forces in the linear bearings of the compliant linkage are negligible in relation to the traction forces between the vehicles' wheels and the ground). A linear encoder measures the momentary distance between the two trucks, and two absolute rotary encoders measure the rotation of the trucks relative to the compliant linkage. Each of the four drive wheels in the system has a shaft encoder to allow conventional dead reckoning.

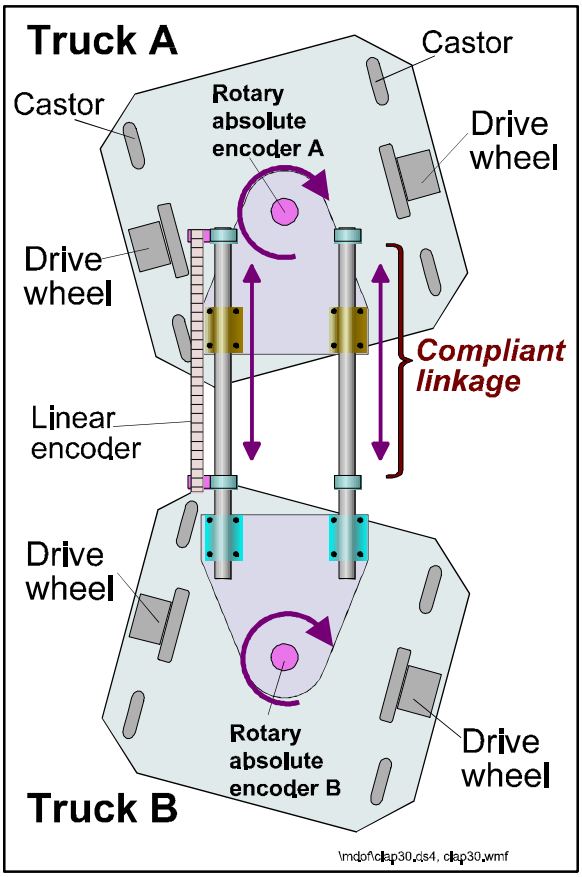

Figure 2: The compliant linkage allows relative motion between the two trucks, to accommodate momentary controller errors. This design eliminates the exessive wheel slippage found in other MDOF vehicles.

The linear incremental encoder has a resolution of 0.1 mm, but the actual accuracy of distance measurements between the centerpoints of the two trucks is only ±3 mm, because of mechanical inaccuracies in our prototype vehicle. The resolution of the rotary absolute encoders is $2^{-10} = 360^{o}/1024 = 0.35^{o}$. We will call these the three *"internal"* encoders.

The experiments with our MDOF vehicle [Borenstein, 1994V1] showed that control errors are effectively absorbed by the compliant linkage, resulting in smooth and precise motion without excessive wheel slippage. In a series of 4×4 m square path experiments we found typical dead-reckoning errors to be less than 6.5 cm in *x* and *y* direction, and orientation errors were less than ±1 ^{o} [Borenstein, 1994a]. This dead-reckoning accuracy is comparable with that of conventional 2-DOF robots. Of course, these results were obtained on smooth floors without irregularities, and with well calibrated parameters to minimize systematic errors.

3. PROPERTIES OF DEAD-RECKONING ERRORS

In this Section we discuss the characteristics of the two distinct types of dead-reckoning errors found in mobile robot navigation: non-systematic and systematic errors. Also in this section we will introduce the *Growth-Rate Concept* for non-systematic dead-reckoning errors. The IPEC method, introduced in Section 4, makes use of this concept to detect and correct non-systematic errors. Section 5 discusses the effect of the IPEC method on systematic errors.

3.1 Non-systematic dead-reckoning errors

Non-systematic errors are usually caused by *irregularities* or roughness of the floor. The surfaces of typical concrete or asphalt floors are strewn with cracks, bumps, and sometimes debris, along with the inherent roughness of the surface. Non-systematic dead-reckoning errors may also be caused by excessive wheel slippage, for example due to a fluid spill. These error sources can neither be avoided nor can they be compensated for with conventional dead-reckoning.

In this section we investigate the properties of a typical non-systematic dead-reckoning error and we develop a numeric example that will be used throughout this paper.

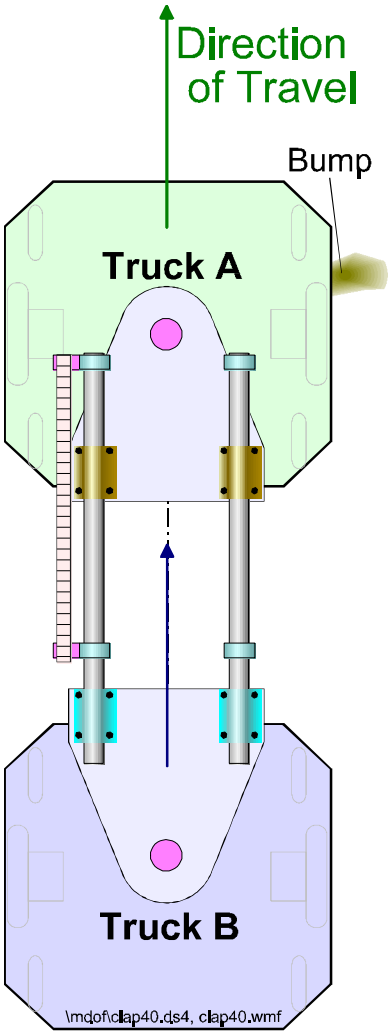

Figure 3: In the initial configuration both trucks are aligned before truck A reaches a bump.

At first, let us assume that both trucks are longitudinally aligned and travel forward, as shown in Fig. 3. For the sake of the numeric example, we will further assume that both trucks are traveling at $V = 0.5$ m/s, and that the sampling time of the *internal encoders* is $T_s = 40$ ms. Thus, during a sampling interval both trucks travel a distance $D_s = VT_s = 20$ mm.

Next, we consider the geometry of a wheel of radius R traversing a bump of height h (see Fig. 4). Making the simplifying assumption that the wheel was perfectly rigid, the wheel will traverse the bump by rotating around the point of contact C until the wheel's center point O is right above C (at O'). During this motion the wheel encoder measures a rotation α, which is interpreted as the linear travel distance D_{meas}. Yet, the actual travel distance in *horizontal* direction is only D_{hor}. This discrepancy creates a linear error ΔD (not shown in Fig. 4):

$$\Delta D = 2(D_{meas} - D_{hor}) \qquad (1)$$

Note that the factor '2' is used because the wheel travels up *and down* the bump.

It is worthwhile at this time to derive a few simple expressions for some other parameters, in order to get a sense for typical dead-reckoning errors. Considering triangle OPC in Fig. 4 we can derive an expression for the *actual* horizontal travel distance

$$D_{hor} = \sqrt{R^2 - (R-h)^2} = \sqrt{2Rh - h^2} \tag{2}$$

Similarly, we approximate from triangle OO`P the *measured* travel distance

$$D_{meas} \approx \sqrt{D_{hor}^{\ 2} + h^2} \tag{3}$$

Note that this approximation is valid for $R >> h$.

For straight-line motion, the low-level controller of a conventional differential-drive mobile robot will try to keep the rotational velocities of both wheels equal. Thus, the *horizontal* distance traveled by the wheel that traversed the bump (the right wheel in the example in Fig. 3) will be ΔD less than that of the left wheel, causing a curved motion to the right, as shown in Fig. 5. After traversing the bump, the vehicle will continue in straight-line motion, but with a constant orientation error $\Delta\theta_a$ (see Fig. 5)

$$\Delta\theta_a \cong \sin^{-1}(\Delta D/b) \tag{4}$$

It is important to note that $\Delta\theta_a$ is the *most significant error* in the system [Feng et al, 1993], because it will cause an ***unbounded*** lateral error, e_{lat}, which grows proportionally with distance at a rate of

$$e_{lat}(D) \cong D \cdot \Delta D/b \cong D \sin \Delta\theta_a \tag{5}$$

where
D - distance traveled since clearing the bump;
b - wheelbase

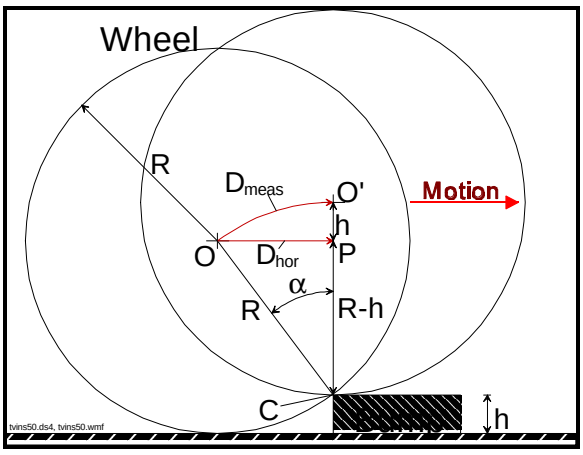

Figure 4: Simplified geometry of a wheel traversing a bump.

In order to get a better sense for the significance of the different components that make up the overall dead-reckoning error, let us consider the typical numeric values in Table I. The physical dimensions b and R correspond to those of the commercially available *LABMATE* robot [TRC]. Substituting b = 340 mm and R = 75 mm, as well as h = 10 mm for a typical bump, into Eqs. (2) and (3) and the results into Eq.

Table I: Sample path errors after traversing a bump

Physical Dimensions			Computed Results		
Wheelbase b	Wheel radius R	Height of bump h	Linear error ΔD	Orientation error $\Delta\theta_a$ (see Fig. 5)	Lateral error after 10m travel e_{lat}(D=10m)
340 mm	75 mm	10 mm	2.63 mm	0.44°	77 mm

(1), we compute the linear error ΔD = 2.63 mm. Then, substituting this value into Eq. (4), we find $\Delta\theta$ = 0.44°. Finally, Using this result in Eq. (5) shows that the lateral error after traveling straight for, say, D = 10 m, is e_{lat} = 77 mm. We will use these sample numbers in the following discussion.

3.2 Systematic dead-reckoning errors

Systematic errors are related to properties of the vehicle, that is, they are independent of the environment. The dominant systematic errors are [Borenstein and Koren, 1985, 1987; Banta, 1988]:

a) Unequal wheel diameters. Mobile robots use rubber tires to improve traction. These tires are difficult to manufacture to exactly the same diameter. Furthermore, rubber tires compress differently under asymmetric load distribution. Both effects can cause substantial dead-reckoning errors.

b) Uncertainty about the wheelbase. The wheelbase is defined as the distance between the contact points of the two drive wheels of a differential drive robot and the floor. The wheelbase must be known in order to compute the number of differential encoder pulses that correspond to a certain amount of rotation of the vehicle. Uncertainty in the effective wheelbase is caused by the fact that rubber tires contact the floor not in one point, but rather in a contact area. the resulting uncertainty about the effective wheelbase can be on the order of up to 5% in some commercially available robots.

In conventional mobile robots systematic errors can be reduced to some degree by careful mechanical design of

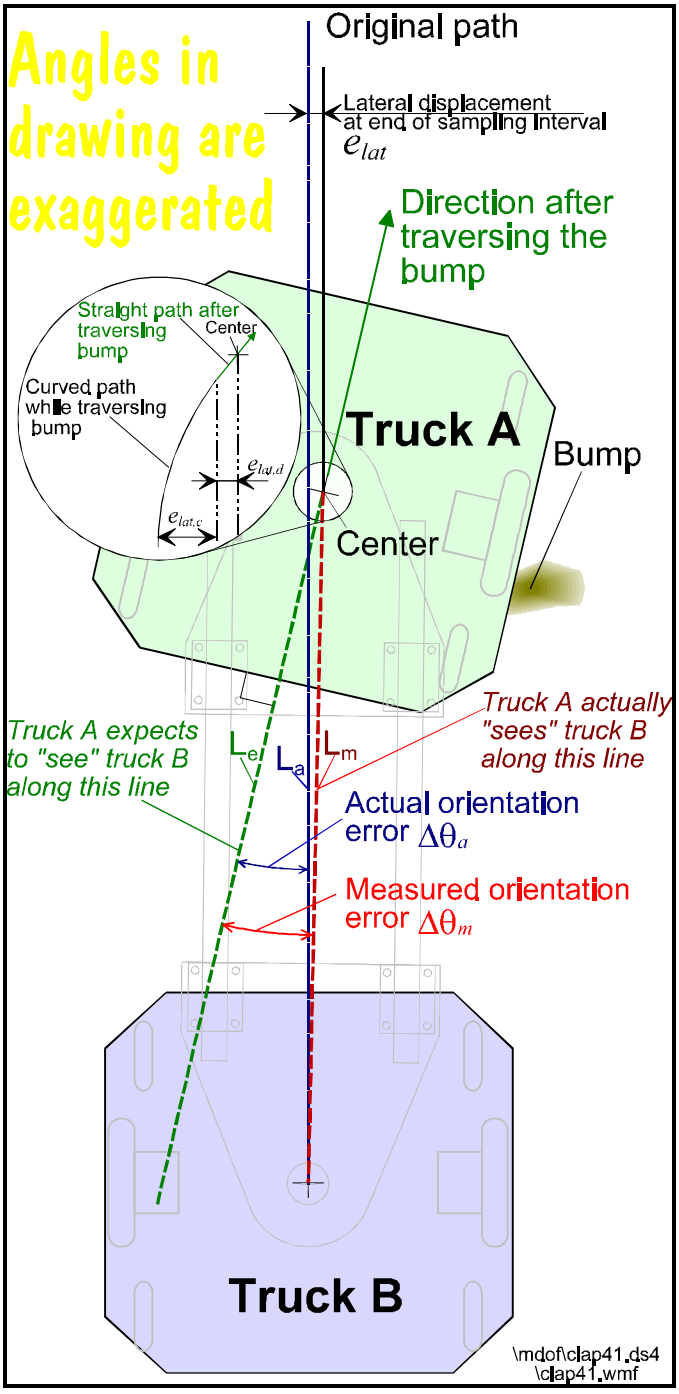

Figure 5: After traversing a bump, the resulting change of orientation of truck A can be measured relative to truck B.

the vehicle and by vehicle-specific calibration. However, systematic errors cannot be completely eliminated since they depend partially on changing factors such as load distribution. Nonetheless, we will see in Section 5 that systematic errors are automatically corrected by the IPEC method, just like non-systematic errors.

3.3 The *Growth-Rate Concept* for dead-reckoning errors

The focus of this paper is *Internal Position Error Correction* (IPEC), a method for the mutual correction of dead-reckoning errors by two linked vehicles. At first glance, it may appear impossible to obtain accurate position corrections from a "floating reference point," such as another vehicle ***in motion***. However, in this section we introduce our new *Growth-Rate Concept* for dead-reckoning errors, which helps overcome the apparent paradox.

The *Growth-Rate Concept* is based on the insight that certain dead-reckoning errors develop quickly (*fast-growing errors)* while others develop slowly (*slow-growing errors*). For example, in a non-holonomous vehicle (such as a differential drive mobile robot) one can safely assume that the vehicle does not move sideways under most normal operating conditions. This holds true even if the vehicle traverses bumps, cracks, or any other irregularity of the floor. Under these "normal" operating conditions, the only way a substantial lateral dead-reckoning error can (and will) develop is as a result of a preceding orientation error. In other words, when the vehicle traverses a bump on the ground, it will *immediately* experience a significant orientation error (thus, a *fast-growing error*), out of which a lateral position error will develop in subsequent travel (a *slow-growing error*).

With the following numeric example we will show that when traversing a bump, (a) each truck can accurately identify the resulting orientation error by measuring its orientation *relative to the other moving truck;* and (b) the lateral position error caused by the same bump is negligible during the same sampling interval.

The enlarged inset in Fig. 5 shows the path of truck A while traversing a bump. Two factors contribute to the resulting lateral position error of truck A: (a) a *curved* section, denoted $e_{lat,c}$, which was generated *while* the wheel was traversing the bump, and (b) a *straight* section, denoted $e_{lat,d}$, which results from the constant directional error *after* traversing the bump. $e_{lat,d}$ is easy to compute, because it is proportional to the travel distance *D after* traversing the bump, and it increases at a constant rate as shown in Eq. (1). However, the trajectory of the truck *while* traversing the bump is difficult to express mathematically, because the orientation error changes during this transient period and it is a function of the geometry of the bump. In this paper we don't need to compute the lateral position error — we only wish to show that it is negligible. For this purpose it is sufficient to determine a reasonable upper bound for $e_{lat,c}$, denoted $e_{lat,max}$, and show that $e_{lat,max}$ is negligible. One (very conservative) upper bound for $e_{lat,c}$ is based on the assumption that the lateral error developed along a straight line, and that the slope of this line resulted from the *largest orientation error during the sampling interval*, denoted $\Delta\theta_{s,max}$. We also note that for the case of a single bump, the orientation error increases monotonously *while* traversing the bump. For example, the orientation error may increase while the wheel rolls up the bump, or it may stay constant while the wheel is on top of the bump, but it won't decrease. Thus, any time we sample the

orientation error, we can be sure it is the largest orientation error since the bump was first encountered (i.e., $\Delta\theta_s \equiv \Delta\theta_{s,max}$). This holds true even if the bump was not yet cleared at the end of the sampling interval.

With this explanation in mind, the *upper bound* for the lateral error while traversing a bump can be determined as

$$e_{lat,max}(D_s) = D_s \sin(\Delta\theta_{s,max}) \tag{6}$$

where D_s is the distance traveled during the sampling interval.

We recall that in the numeric example of Section 3.1 D_s = 20 mm and $\Delta\theta_{s,max} \equiv \Delta\theta_s$ = 0.44°. Substituting these values into Eq. (6) yields an upper bound of $e_{lat,max}(D_s)$ = 0.15 mm.

Note that the upper bound for the curved segment in Eq. (6) is exactly equal to the lateral error caused by the straight section (i.e., $e_{lat,max}(D_s) = e_{lat,d}$). Thus, the maximum lateral error during a sampling interval is always given by Eq. (6), and it doesn't matter if at the end of the sampling interval the robot was still traversing or had already cleared the bump.

Next, we will show that the lateral error has no significant influence on the accuracy of the relative orientation measurement between the two trucks. Given that the CLAPPER maintains a distance of L = 1 m between the two trucks, one can easily compute from the geometry of Fig. 5 that the maximum lateral error $e_{lat,max}(D_s)$ = 0.15 mm will reduce the *actual* orientation error $\Delta\theta_a$ = 0.76° by

$$\epsilon = \text{asin}(e_{lat,max}(D_s)/L) = \text{asin}(0.15/1000) = 0.01^\circ \tag{7}$$

and result in a *measured* orientation error

$$\Delta\theta_m = \Delta\theta_a - \epsilon = 0.44^\circ - 0.01^\circ = 0.43^\circ \tag{8}$$

Thus, even the maximum lateral error $e_{lat,max}$ affects the accuracy of the orientation error measurement only by ϵ = 0.01° or 0.01/0.43×100 = 2.3%.

This numeric example illustrates the *Growth-Rate Concept* for dead-reckoning errors: The 10 mm bump in our example causes an appreciable and immediately measurable orientation error of $\Delta\theta_a$ = 0.44°, while the resulting lateral error e_{lat} = 0.15 mm remains negligibly small during a reasonably short sampling interval and reduces the accuracy of the orientation measurement by only 2.3%.

So far, we have examined the most basic case in which only truck A encountered a bump while truck B retained its heading. However, even if truck B also encountered a bump *during the same sampling interval*, its lateral error would be similarly small. Neither this lateral error nor the orientation error of truck B would cause a significant error in the orientation measurement of truck A relative to B or vice versa. Yet, even in this extreme and rare case, the

inaccuracy of the orientation error measurement would be $\epsilon = 2\times0.01^{o} = 0.02^{o}$, which translates into 0.02/0.44×100 = 4.5% inaccuracy in measuring the orientation error of truck A relative to truck B.

4. INTERNAL POSITION ERROR CORRECTION (IPEC)

The principle of operation of the IPEC method is best explained with the help of Fig. 5, which shows truck A's "direction of travel after traversing a bump." Since this direction differs from the intended (straight ahead) direction as the result of a dead-reckoning error, truck A still "believes" it was traveling straight ahead. Consequently, truck A would expect the center of truck B straight behind, along the dotted line labeled L_e in Fig. 5. Using dead-reckoning data from both trucks, truck A can always compute this *expected direction* to the center of truck B, whether both trucks are traveling straight or along a curved path. This *expected* direction can then be compared to the *measured* direction, which is readily available from the absolute rotary encoder on truck A. The difference between the *expected* direction and the measured direction is the *measured* orientation error $\Delta\theta_m$. The orientation error of truck B can be determined in a similar way, relative to the center of truck A.

4.1 Correction of orientation errors

In this section we explain the actual implementation of the IPEC method on the CLAPPER. With its three *internal* encoders, the CLAPPER performs relative position measurements every T_s = 40 ms. This sampling rate allows each truck to detect the *fast-growing* orientation errors caused by bumps. The *slow-growing* lateral position errors of both trucks have no significant effect on this measurement, as was shown in Section 3. Note that the sampling time is not critical for the performance of the system.

The IPEC method performs the following computations once during each sampling interval: At first, trucks A and B compute their momentary position and orientation based on dead-reckoning:

$$\begin{aligned} x_{A,i} &= x_{A,i-1} + U_{A,i}\cos\theta_{A,i} \\ y_{A,i} &= y_{A,i-1} + U_{A,i}\sin\theta_{A,i} \end{aligned}$$

and (9)

$$\begin{aligned} x_{B,i} &= x_{B,i-1} + U_{B,i}\cos\theta_{B,i} \\ y_{B,i} &= y_{B,i-1} + U_{B,i}\sin\theta_{B,i} \end{aligned}$$

where

$x_{A,i}$, $y_{A,i}$ - position of centerpoint of truck A, at instant i;
$x_{B,i}$, $y_{B,i}$ - position of centerpoint of truck B, at instant i;
$U_{A,i}$, $U_{B,i}$ - incremental displacements of the centerpoints of trucks A and B during the last sampling interval;
$\theta_{A,i}$, $\theta_{B,i}$ - Orientations of trucks A and B, respectively; computed from dead-reckoning.

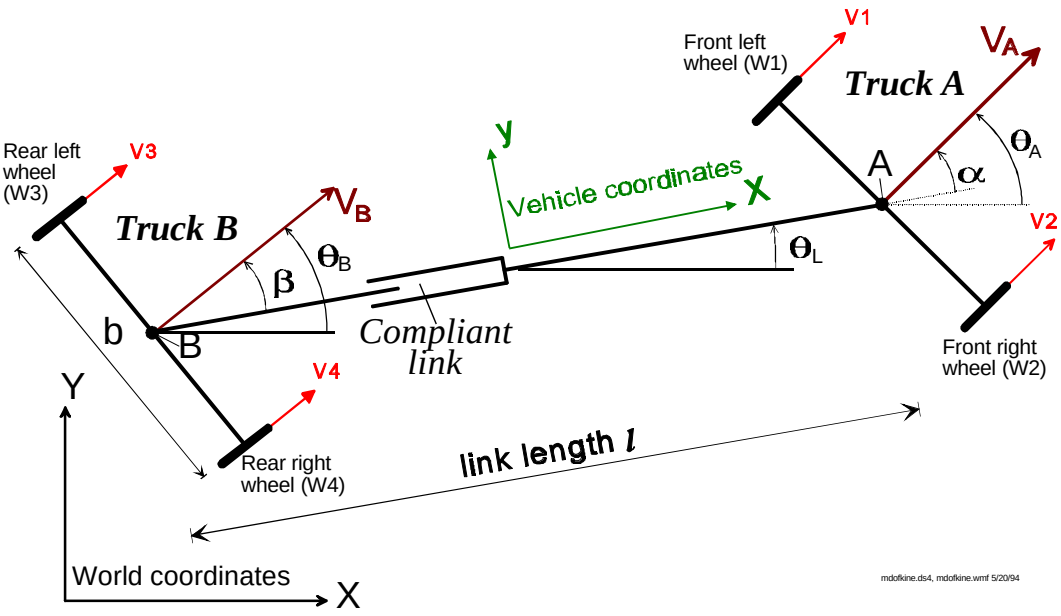

Figure 6: Kinematic definitions for the CLAPPER.

Note that the dead-reckoning equations for U_i and θ_i are well known and not repeated here (see [Banta, 1988; Everett, 1995]). Also note that we will skip the index i in the following equations.

Next, the orientation θ_L of the compliant linkage is computed

$$\theta_L = \text{atan}\left(\frac{y_B - y_A}{x_B - x_A}\right) \tag{10}$$

Using the kinematic relations defined in Fig. 6, we can now compute the *expected* angles α_{exp} and β_{exp} between the compliant linkage and trucks A and B respectively.

$$\alpha_{exp} = \theta_A - \theta_L \tag{11a}$$

and

$$\beta_{exp} = \theta_B - \theta_L \tag{11b}$$

Note that the index "*exp*" indicates that the computed angle is ***expected***, based on dead-reckoning during this sampling interval.

We can now compute

$$\Delta\theta_A = \alpha_{act} - \alpha_{exp} \tag{12a}$$

and

$$\Delta\theta_B = \beta_{act} - \beta_{exp} \tag{12b}$$

where α_{act} and β_{act} are the ***actual*** angles between the compliant linkage and trucks A and B respectively, as measured by the two absolute rotary encoders located at points A and B (see

Fig. 2 and Fig. 6). Non-zero results for $\Delta\theta_A$ or $\Delta\theta_B$ do not only indicate the presence of a dead-reckoning error, but they are quantitatively accurate values for correcting these errors. Thus, computing

$$\theta'_A = \theta_A + \Delta\theta_A \quad (13a)$$

and

$$\theta'_B = \theta_B + \Delta\theta_B \quad (13b)$$

yields the *corrected* orientations for truck A and truck B.

4.2 Correction of translational errors

The IPEC method can detect only rotational errors, but not translational errors. However, rotational errors are much more severe than translational errors, because orientation errors cause ***unbounded*** growth of lateral position errors. This observation was illustrated in Table I, where the translational error resulting from traversing a bump of height 10 mm was ΔD = 2.63 mm. By comparison, the lateral error due to the rotational error $\Delta\theta$ was e_{lat} = 77 mm after only 10 m of travel.

We can further distinguish two kinds of translational errors: *pure* and *composite*. *Pure* translational errors occur when both wheels traverse bumps of similar height during the same sampling interval. These errors cannot be detected with the IPEC method, but they are rare in practice and they produce only small and finite position errors. *Composite* translational errors occur when only one wheel traverses a bump, thereby causing a translational ***and*** a rotational error. Since we can detect the rotational error, we can also correct for the translational part, as discussed next.

Since *composite* translational dead-reckoning errors are the result of a rotation (the magnitude of which is known from Eqs. (12)), it is possible to correct the translational error once we know the point around which the rotation took place. Banta [1988] helps solve this problem by explaining that a non-systematic orientation error is practically ***always*** caused by an encoder reporting a horizontal distance that is ***longer*** than the distance the wheel had actually traveled. This is true for all kinds of floor irregularities, whether they are bumps, cracks, or fluid spills. Because of this important insight we can safely assume that the dead-reckoning orientation error of $\Delta\theta_a = 0.44^o$ (in our example) is not caused by the left wheel that has progressed more than reported by the encoder — rather, it is the right wheel that has lagged behind in its horizontal progression although the (false) encoder readings make the robot believe both wheels had progressed the same horizontal distance. We can thus correct the internal position representation of truck A by applying the corrective rotation $\Delta\theta_A$ around the contact point of the left wheel, so that the position of the centerpoint A is corrected backward (see Fig. 7) by

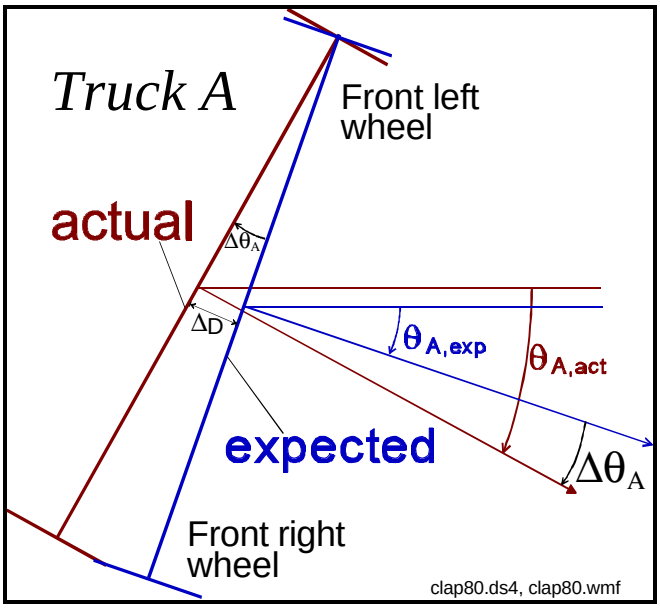

Figure 7: Correcting *composite* translational errors.

$$\Delta D = b \sin(\tfrac{1}{2}\Delta\theta_A) \qquad (14)$$

or

$$x'_A = x_A - b \sin(\tfrac{1}{2}\Delta\theta_A)\cos(\theta_A)$$
$$y'_A = y_A - b \sin(\tfrac{1}{2}\Delta\theta_A)\sin(\theta_A) \qquad (15)$$

In actual experimentation we found that this correction of the translational error has only minimal effect on the overall accuracy of the system. By contrast, the position correction for truck B is of crucial importance, and it must be done in a different manner and for different reasons, as explained next.

It is clear at this time that the IPEC method does not eliminate dead-reckoning errors *completely*. Thus, after some travel time both trucks will have accumulated a certain position error. Yet, even the smallest position error of either truck will affect the computation of the orientation θ_L of the compliant linkage. Such an error in θ_L, in turn, would affect Eqs. (11), causing the system to "see" and correct non-existing dead-reckoning errors all the time. To avoid this problem, we have to correct the position of one truck relative to the other after every sampling interval. In our case, we correct the position of truck B according to

$$x'_B = x_A - l\cos\theta_L$$
$$y'_B = y_A - l\sin\theta_L \qquad (16)$$

where x'_B, y'_B are the corrected coordinates of truck B, and l is the length of the compliant linkage, as measured by the linear encoder onboard the CLAPPER.

The effect of this correction is that the position of truck B is not at all computed by summing-up dead-reckoning increments. Rather, truck B's dead-reckoning is relevant only for the distance traveled during one sampling interval, while its accumulated position is always computed relative to truck A. This measure is perfectly legitimate because the position of truck B relative to truck A can always be computed from the three internal encoders. The single disadvantage is the need to measure the distance between the trucks (l) quite accurately, to avoid systematic errors during turning (as we will discuss in Section 5).

5. SYSTEMATIC DEAD-RECKONING ERRORS

In Section 4 we explained the IPEC method with regard to non-systematic errors. Another source of dead-reckoning errors is known as *systematic errors*. Systematic errors are usually caused by imperfections in the design and mechanical implementation of a mobile robot. In conventional, differential-drive mobile robots the two most notorious systematic errors are different wheel diameters and the uncertainty about the effective wheelbase [Borenstein and Koren, 1985, 1987; Banta 1988; Borenstein and Feng, 1995].

Systematic errors are particularly grave, because they accumulate constantly. On most smooth indoor surfaces systematic errors contribute much more to dead-reckoning errors than non-systematic errors. However, on rough surfaces with significant irregularities, non-systematic errors are dominant. One hard-to-defuse criticism of work aimed at reducing systematic dead-reckoning errors alone is the claim that any *unexpected* irregularity can introduce a huge error, no matter how effective the reduction of systematic errors was.

5.1 Correction of conventional systematic errors with the CLAPPER

The IPEC method corrects not only non-systematic errors, but it can also compensate for most systematic errors, provided the systematic error causes a dead-reckoning error in orientation. For example, consider a mobile robot programmed to move straight ahead. Unequal wheel-diameters will cause the mobile robot to follow a curved path, instead. Even though the resulting rate of rotation is very small, the CLAPPER will trigger a correction as soon as the accumulated orientation error exceeds the resolution of the absolute encoder (0.3 ^{o} in the CLAPPER). In our experiments we found that the CLAPPER can easily accommodate and correct large systematic errors. Indeed, we have implemented a calibration procedure in which certain systematic errors (like unequal wheel-diameters) are automatically calibrated by monitoring the corrective actions of the CLAPPER while traveling on smooth surfaces. Similarly, the error resulting from the uncertainty about the effective wheelbase of the trucks can be corrected with the IPEC method.

5.2 Unconventional systematic errors in the CLAPPER

While the CLAPPER corrects most systematic errors of *conventional* mobile robots, the vehicle introduces new *unconventional* systematic errors that are specific to the CLAPPER. These *unconventional* systematic errors are related to (a) biased measurements of the absolute rotary encoders, and (b) biased measurements of the link-length l. Consider, for example, the situation in which the CLAPPER is programmed to move straight ahead. The onboard controller will comply with this task by controlling both trucks such that both absolute encoders don't deviate from $\alpha = \beta = 0^{o}$. Now suppose that because of inaccurate assembly of the vehicle encoder A reads 0 ^{o} while truck A is actually rotated, say, +1 ^{o} relative to the compliant linkage. Suppose further encoder B showed 0 ^{o} while truck B was actually rotated -1^{o} relative to the compliant linkage. The resultant path would be curved to the left instead of straight. This condition cannot be detected by the IPEC method and its effect is similar to that of unequal wheel-diameters in conventional mobile robots.

Another unconventional systematic error is related to the biased measurement of the linear encoder. Even though the resolution of this encoder in our prototype vehicle is 0.1 mm, we suspect that our prototype vehicle has a constant bias on the order of 2 mm and, in addition, a problem with eccentricity, which changes the bias when the two trucks rotate relative to the compliant linkage. This link-length bias will cause a slight inaccuracy in the correction of the rear-truck position, because Eqs. (16) depend on the link length l. During straight line travel the link-length bias has no effect on the overall accuracy of the system. However, during turning movements any small inaccuracy in the position of the rear truck will cause a small error in computing the orientation of the compliant linkage, θ_L, because of Eq. (10). Such an error will be interpreted by the CLAPPER as a dead-reckoning error during the next sampling interval, because of Eqs. (11). Consequently the CLAPPER will "correct" this perceived dead-reckoning error. In informal experiments we found that a constant bias of 1 mm in the measurement of the link-length l causes an orientation error of roughly 1° for every full 360° turn of the CLAPPER. In either case, however, the vehicle can be calibrated to the extend that these errors become negligible, as the experimental results with a well calibrated vehicle will show in Section 6, below.

5.3 Conventional versus unconventional systematic errors

So far we have seen that the CLAPPER corrects most *conventional* systematic errors, while introducing some new, *unconventional* systematic errors of its own. However, we argue that these *unconventional* errors are less of a problem, for the following reasons:

a. The most severe conventional systematic errors depend to a large degree on circumstances that can not be controlled by the robot's manufacturer. For example, unequal wheel-diameters are often the result of different loading characteristics of the vehicle. By contrast, the unconventional systematic errors of the CLAPPER depend on fixed manufacturing characteristics of the vehicle. Being aware of the importance of reducing measurement bias, the manufacturer of a CLAPPER-type vehicle can design and build the vehicle with tight tolerances for the assembly of the encoders.

b. The measurement bias of the absolute encoders in the CLAPPER can be detected and corrected by means of simple calibration procedures. Once these procedures have been performed, the resulting calibration parameters remain basically valid under all operating conditions, independent of floor or load characteristics.

6. EXPERIMENTAL RESULTS

In order to evaluate the performance of the CLAPPER's IPEC method we conducted several sets of representative experiments. In this section we report results from repeatable, basic experiments inside the lab. Results from other experiments, including runs on a bumpy lawn, are documented in [Borenstein, 1995V].

All indoor experiments were conducted on fairly smooth concrete floors. We produced controlled irregularities by repeatedly placing a piece of 10 mm diameter cable under one side of the vehicle. We will refer to this irregularity as a "bump." All experiments started and ended near an L-shaped reference corner. Three ultrasonic sensors were mounted on the CLAPPER, two sensors were facing the long side of the L-shaped corner, the third sensor faced the short side. The ultrasonic sensor system allowed measurement of the absolute position of the vehicle to within ±2 millimeters in the *x* and *y* directions, and to about ±0.25 ° in orientation.

At the beginning of each run a sonar measurement was taken to determine the starting position of the vehicle. The CLAPPER then traveled through the programmed path and returned to the L-shaped corner, where the *perceived* position (i.e., the position the vehicle "thought" it had, based on dead-reckoning) was recorded. Then, a sonar measurement was taken to determine the *absolute* position. The difference between the absolute position and the perceived position is called the *return position error*. The average speed in all runs was slightly below 0.5 m/sec.

6.1 The *Straight Line Experiment*

In this experiment the CLAPPER traveled straight forward for 18 m, stopped, and returned straight-backward for 18 m, to the starting position. We performed three runs for each one of the following four conditions:

a. Without IPEC, without bumps
b. Without IPEC, with ***ten*** bumps
c. With IPEC, without bumps
d. With IPEC, with ***twenty*** bumps

In the runs "without bumps" one can assume disturbance-free motion because our lab has a fairly smooth concrete floor. In the runs "with bumps" we used bumps only on the return leg of the 2×18 m round-trip and only under the right side-wheels of the vehicle (to avoid mutual cancellation of errors). In the runs with error correction we used 20 bumps approximately evenly spaced along the 18 m return-path. Some bumps affected both the front and rear truck, some affected only one of the two trucks. In the runs without error correction we used only 10 bumps, because our cluttered lab could otherwise not accommodate the large

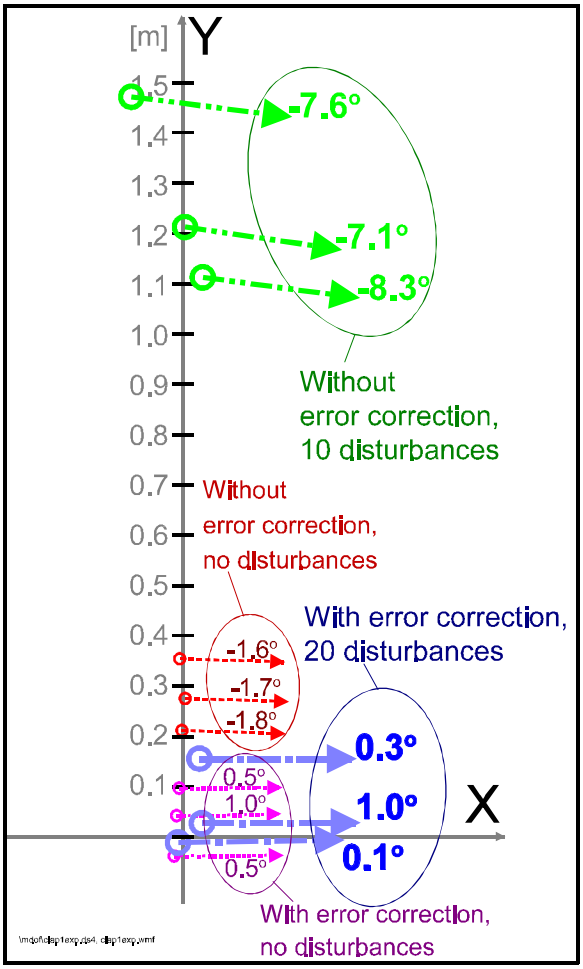

Figure 8: Return position errors after completing the *Straight Path Experiment*.

path deviations. Without error correction, each bump caused an orientation error of approximately $\epsilon_\theta = 0.6^o$.

Figure 8 summarizes the results from the straight-line experiment. Shown are the return position errors and the return orientation errors of the vehicle after completing the 36 m journey back and forth along the x-axis. Note that without bumps, the return position errors with IPEC are only slightly smaller than those without IPEC. We contribute the almost uniform orientation error of approx. -1.7 ^{o} in the run without IPEC to conventional systematic errors. The run with IPEC shows how the conventional systematic errors are overcome. The more important results are those from runs with bumps. Here the non-IPEC runs average a return orientation error of $\epsilon_{\theta,avrg} = -7.7^o$, out of which -1.7 ^{o} are likely to be the result of systematic errors. The remaining error average of $\epsilon_\theta = -6^o$ can be interpreted as the result of the 10 identical bumps, each of which contributed 0.6 ^{o}.

We performed many more straight line experiments than the ones documented here. In all runs the return orientation error ϵ_θ with IPEC was less than ±1.0 ^{o} for the 36 m straight line path.

6.2 The *Rectangular Path Experiment*

In this experiment the CLAPPER was programmed to pass-by the corners of a 7×4 m rectangular path with smooth 90 ^{o} turns at the corners and a total travel length of approximately 24 m (see Fig. 9). To provide fluid, uninterrupted motion, the programmed path did not require the vehicle to stop at the intermediate points — passing-by at a distance of less than 0.2 m was sufficient. In order to measure the position errors after completing the path, the vehicle began and ended each run in the L-shaped "home" corner, as shown in Fig. 9.

When testing dead-reckoning errors in closed-path experiments, it is imperative to run the experiment in both clockwise (cw) and counter-clockwise (ccw) directions. If tests are run in only one direction (for example, to calibrate parameters that determine the effective wheelbase or compensate for different wheel-diameters), then systematic dead-reckoning errors can mutually compensate for each other. This way, an experimenter might carefully calibrate two parameters to yield excellent accuracy for a particular test-path, yet the calibrated parameters are quite wrong. If, however, the test is performed in both cw and ccw direction, then mutual compensation in one direction increases the resulting error when run in the other direction. Thus, if a mobile robot performs a closed test path accurately in both directions, one can be assured that the vehicle is well calibrated.

Figure 10 shows the return position errors for the *Rectangular Path Experiment* under different test conditions. The CLAPPER ran through the path for 10 runs in cw, and 10 runs in ccw direction. In each of these runs the CLAPPER had to traverse 10 bumps. In one half of the runs bumps were located under the right-side wheels of both trucks, and in the other half of the runs under the left-side. The return position errors of these runs are marked by small squares (see *Legend* in Fig. 10). None of the 20 runs produced a position error of more than 5 cm. Also shown in Fig. 10 are the results of five cw and five ccw runs with IPEC but

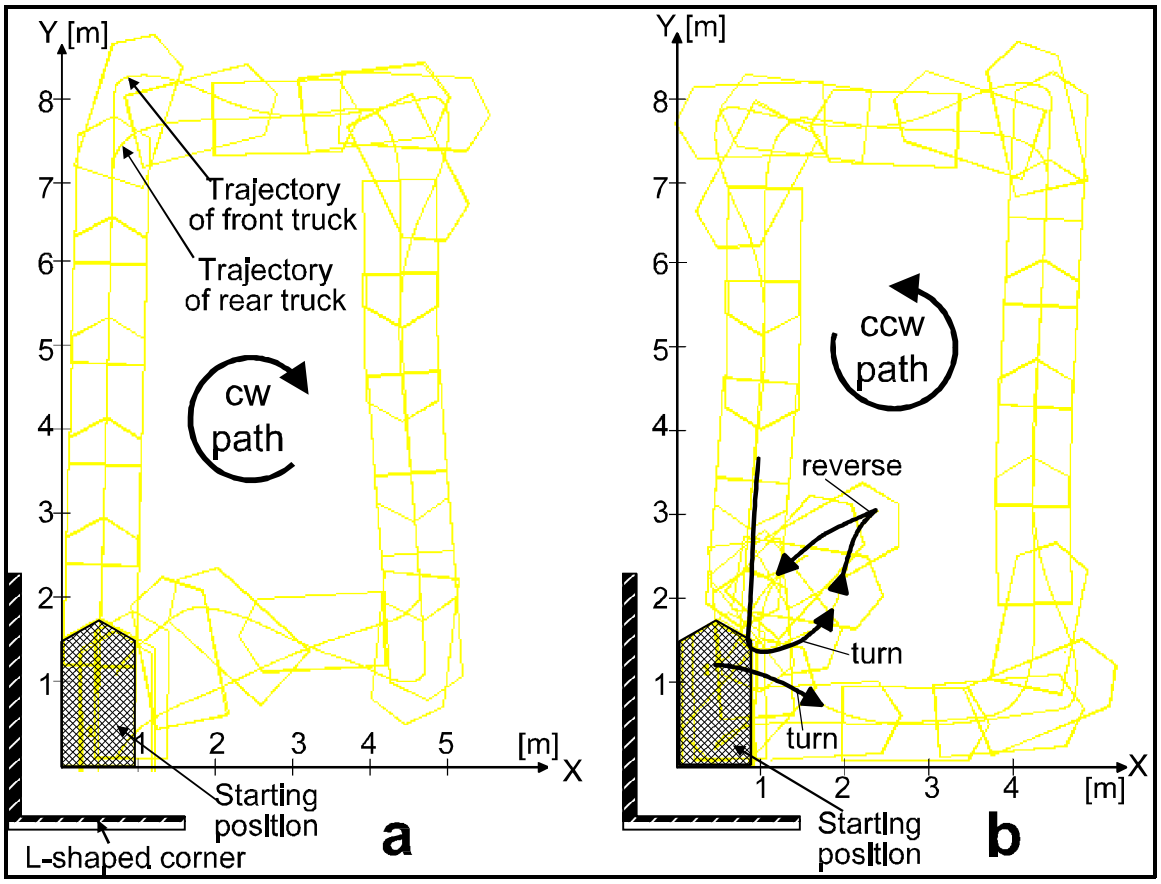

Figure 9: The *Rectangular Path Experiment* was performed in clockwise (cw) and counter-clockwise (ccw) direction. Some sideways and backward maneuvering was necessary to return to the home position.

without bumps (marked by small circles). Note that the results with bumps are almost indistinguishable from the results without bumps. In a further experiment the vehicle ran through the path with bumps, while the IPEC function was *disabled* (i.e., using normal dead-reckoning like conventional mobile robots). The results of these runs are marked by stars in Fig. 10. Also noted in the inset table in Fig. 10 are the resulting *average absolute orientation errors* of these runs, defined as

$$\epsilon_{\theta,|avrg|} = \frac{1}{n}\sum_{i=1}^{n} |\epsilon_{\theta,i}| \qquad (17)$$

One might recall that for longer distances the orientation errors cause the lateral position errors to grow without bound. The results in Fig. 10 show that the IPEC method resulted in a more than 20-fold reduction in orientation errors. Indeed, in longer paths with more disturbances one should expect even better improvements, because the average absolute orientation error of $\epsilon_{\theta,avrg} = 0.3^o$ is just about equal to the accuracy with which we are able to measure the actual position of the CLAPPER with the three onboard ultrasonic sensors.

These experimental results compare well with experimental results obtained by the author in earlier work [Borenstein, 1994a] with the same MDOF vehicle but without IPEC. In those experiments the average translational error in 10 runs along a 4×4 m rectangular path was $\epsilon_{max} = 5.6$ cm and the average absolute orientation error was approximately 0.7 °. These earlier experiments, of course, were conducted on smooth floors with a well calibrated vehicle. The improvement evident in the results of Fig. 10 over the earlier, non-IPEC results on smooth floors can be accredited to the ability of the IPEC method to correct not only non-systematic dead-reckoning errors but also conventional systematic errors. These results further indicate that careful calibration of the non-conventional system parameters in the CLAPPER is more effective than the equally careful calibration of conventional system parameters in conventional vehicles.

7. CONCLUSIONS, APPLICATIONS, AND FUTURE WORK

A new method for *Internal Position Error Correction* (IPEC) for mobile robots has been developed. The IPEC method has been implemented and tested on the University of Michigan's Multi-Degree-of-Freedom (MDOF) vehicle called CLAPPER. The main strength of the new method is the immediate correction of both systematic and non-systematic dead-reckoning errors without external references and during motion. Experimental results with the

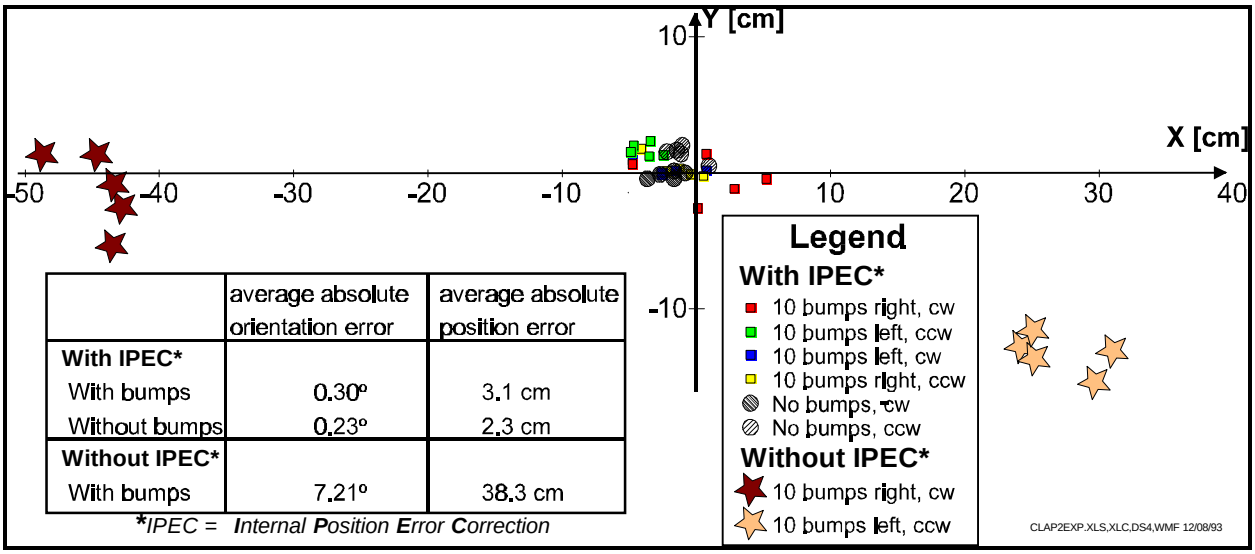

	average absolute orientation error	average absolute position error
With IPEC*		
With bumps	0.30°	3.1 cm
Without bumps	0.23°	2.3 cm
Without IPEC*		
With bumps	7.21°	38.3 cm

**IPEC = Internal Position Error Correction*

Figure 10: Return position errors after completing the *Rectangular Path Experiment.* Total travel distance in each run: 21m.

CLAPPER show one to two orders of magnitude more accurate dead-reckoning than conventional (2-DOF) mobile robots. Thus, the CLAPPER not only eliminates the excessive wheel slippage found in other MDOF vehicles, but it corrects dead-reckoning accuracy even further, for a total improvement of two to three orders of magnitude over other MDOF vehicles.

The CLAPPER is especially suitable for industrial applications where its unique dead-reckoning accuracy will allow it to operate without the guide-wires typically found in conventional AGV applications. The IPEC method is also useful in applications where substantial floor irregularities or the mere possibility for unexpected floor irregularities render conventional dead-reckoning unfeasible. Construction and agricultural applications, where dead-reckoning has been impossible in the past because of the large amount of slippage on soft soil, might benefit directly from the IPEC method. Other relevant applications are map-building and exploratory tasks, where conventional absolute position sensors are unfeasible.

We have just begun to investigate the applicability of the IPEC design to other vehicle configurations. One promising approach is the attachment of an unpowered *encoder trailer* to existing, conventional mobile robots. Linking this *encoder trailer* with one rotary joint to the main vehicle would produce a configuration similar to the CLAPPER's, except for the fact that the *encoder trailer*, acting as truck B, would be passively towed instead of being motorized. Simulations results with such an encoder trailer were encouraging [Borenstein, 1994c] and we have recently begun building the actual device. Results are expected in early 1995.

We are also considering the possibility of using the IPEC method on two collaborating but physically unconnected mobile robots. Both robots would have to be equipped with positioning sensors capable of accurately measuring the relative position and bearing between the two units. This approach may be useful for tracked vehicles in military, agricultural, or construction applications.

Acknowledgements:

This research was funded by NSF grant # DDM-9114394 and in part by Department of Energy Grant DE-FG02-86NE37969.

Special thanks to Dr. Liquiang Feng who provided comments and suggestions in the review of this manuscript and to Mr. Dilip Dubey who conducted some of the experiments.

---

8. REFERENCES

1. Banta, L., 1988, "A Self Tuning Navigation Algorithm." *Proceedings of the 1988 IEEE International Conference on Robotics and Automation*, Philadelphia, April 25, pp. 1313-1314.

2. Barshan, B. and Durrant-Whyte, H.F., 1993, "An Inertial Navigation System for a Mobile Robot." *Proceedings of the 1st IAV*, Southampton, England, April 18-21, 1993, pp. 54-59.

3. Borenstein, J. and Koren, Y., 1985, "A Mobile Platform For Nursing Robots." *IEEE Transactions on Industrial Electronics*, Vol. 32, No. 2, pp. 158-165.

4. Borenstein, J. and Koren, Y., 1987, "Motion Control Analysis of a Mobile Robot." *Transactions of ASME, Journal of Dynamics, Measurement and Control*, Vol. 109, No. 2, pp. 73-79.

5. Borenstein, J., 1993, "Multi-layered Control of a Four-Degree-of-Freedom Mobile Robot With Compliant Linkage." *Proceedings of the 1993 IEEE International Conference on Robotics and Automation*, Atlanta, Georgia, May 2-7, pp. 3.7-3.12.

6. Borenstein, J., 1994a, "Control and Kinematic Design for Multi-degree-of-freedom Mobile Robots With Compliant Linkage." *IEEE Transactions on Robotics and Automation*, Vol. 11, No. 1, February 1995, pp. 21-35..

7. Borenstein, J., 1994b, "The CLAPPER: a Dual-drive Mobile Robot With Internal Correction of Dead-reckoning Errors." *Proceedings of the 1994 IEEE International Conference on Robotics and Automation*, San Diego, CA, May 8-13, 1994, pp. 3085-3090.

8. Borenstein, J, 1994c, "Internal Correction of Dead-reckoning Errors With the Smart Encoder Trailer." *1994 International Conference on Intelligent Robots and Systems (lROS '94)*. München, Germany, September 12-16, 1994, pp. 127-134.

9. Borenstein, J., 1994V1, "Four-Degree-of-Freedom Redundant Drive Vehicle With Compliant Linkage." ***Video Proceedings*** *of the 1994 IEEE International Conference on Robotics and Automation*, San Diego, CA, May 8-13, 1994 (Note: The Video Proceedings booklet lists this entry under incorrect title and abstract).

10. Borenstein, J., 1995V2, "The CLAPPER: A Dual-drive Mobile Robot With Internal Correction of Dead-reckoning Errors." *Accepted for the Video Proceedings of the 1995 IEEE International Conference on Robotics and Automation*, Japan, May, 1995.

11. Borenstein J. and Feng. L, 1995, "Measurement and Correction of Systematic Dead-reckoning Errors in Mobile Robots.." Submitted to the *IEEE Journal of Robotics and Automation*, November 1994.

12. Byrne, R.H., 1993, "Global Positioning System Receiver Evaluation Results." Sandia Report SAND93-0827, Sandia National Laboratories, Albuquerque, NM, September, 1993.

13. Congdon, I. et al., 1993, "CARMEL Versus FLAKEY — A Comparison of Two Winners." *AI Magazine Winter 1992*, pp. 49-56.

14. Cox, I. J., 1991, "Blanche — An Experiment in Guidance and Navigation of an Autonomous Robot Vehicle." *IEEE Transactions on Robotics and Automation*, vol. 7, no. 2, April, pp. 193-204.

15. Everett, H.R. "*Sensors for Mobile Robots*," A K Peters, Ltd., Wellesley, expected publication date Spring 1995.

16. Feng, L, Koren, Y., and Borenstein, J., 1993, "A Cross-Coupling Motion Controller for Mobile Robots." *IEEE Journal of Control Systems*. December 1993, pp. 35-43.

17. Gourley and Trivedi, M., 1994, "Sensor Based Obstacle Avoidance and Mapping for Fast Mobile Robots." *Proceedings of the 1994 IEEE International Robotics and Automation*, San Diego, CA, May 8-13, pp. 1306-1311.

18. Hirose, S., and Amano, S., 1993, "The VUTON: High Payload Efficiency Holonomic Omni-Directional Vehicle." Proceedings of the Sixth International Symposium on Robotics Research (ISRR-93), Hidden Valley, PA, Oct. 2-5, 1993.

19. Hongo, T., Arakawa, H., Sugimoto, G., Tange, K., and Yamamoto, Y., 1987, “An Automated Guidance System of a Self-Controlled Vehicle.” IEEE Transactions on Industrial Electronics, Vol. IE-34, No. 1, 1987, pp. 5-10.

20. Kurazume R. and Nagata, S., 1994, "Cooperative Positioning With Multiple Robots." *Proceedings of IEEE International Conference on Robotics and Automation*, San Diego, CA, May 8-13, pp. 1250-1257.

21. Killough, S. M. and Pin, F. G., 1992, "Design of an Omnidirectional Holonomic Wheeled Platform Prototype." *Proceedings of the IEEE Conference on Robotics and Automation*, Nice, France, May 1992, pp. 84-90.

22. Moravec, H. P., 1984, "Three Degrees for a Mobile Robot." Carnegie-Mellon University, *The Robotics Institute*, Mobile Robots Laboratory, Technical Report.

23. Pin, F. G. and Killough, M., 1994, "A New Family of Omnidirectional and Holonomic Wheeled Platforms for Mobile Robots." *IEEE Transactions on Robotics and Automation*, Vol. 10, No. 4, August 1994, pp. 480-489.

24. Reister, D. B., 1991, "A New Wheel Control System for the Omnidirectional HERMIES-III Robot." *Proceedings of the IEEE Conference on Robotics and Automation* Sacramento, California, April 7-12, pp. 2322-2327.

25. Reister, D.B. and Unseren, M.A., 1993, "Position and Constraint Force Control of a Vehicle with Two or More Steerable Drive Wheels." *IEEE Transactions on Robotics and Automation*.Vol. 9, No. 6, December, pp. 723-731.

26. Schiele, B. and Crowley, J., 1994, "A Comparison of Position Estimation Techniques Using Occupancy Grids." *Proceedings of IEEE International Conference on Robotics and Automation*, San Diego, CA, May 8-13, pp. 1628-1634.

27. TRC (Transition Research Corporation), 1993, , Danbury, Connecticut, 06810.

28. West, M. and Asada, H., 1992, "Design of a Holonomic Omnidirectional Vehicle." *Proceedings of the 1992 IEEE International Conference on Robotics and Automation.* Nice, France, May 1992, pp. 97-103.